

Time-Reverse Imaging for the Detection of Landmines

Mubashir Alam*, James H. McClellan*, Pelham Norville, and Waymond R. Scott Jr

*Center of Signal and Image Processing
School of Electrical and Computer Engineering
Georgia Institute of Technology, Atlanta, Georgia 30332-0250

ABSTRACT

Time Reversal is based on the fact that most physical laws of nature are invariant for time reversal, i.e., when time t is replaced by $-t$, most physical laws remain unchanged. Physically this means that by time reversing, a particle will retrace its original path or trajectory. Based on this fact, systems were built which receive reflections or scattering from targets. If this reflected data is recorded, time reversed and launched into the medium again, it will focus back on the targets. This is the basis for experimental time reversal. Time reverse imaging is somewhat different in the sense that scattering from targets are recorded on the sensors, but then back propagated numerically. Narrow-band or single frequency MUSIC based time-reverse imaging algorithms have been proposed in literature for point-like targets. When this algorithm is applied to scattering from an extended target, such as a landmine, the image has good cross-range resolution, but rather poor range resolution. We propose the use of 2-D MUSIC-based algorithm to improve the near-field range resolution, which can then be used in conjunction with single frequency MUSIC to produce a final high-resolution image. A FDTD elastic-wave simulation is used to verify the results using mines and mine-like targets embedded in a heterogenous soil.

Keywords

Time-Reversal, Array Imaging, Seismic, Acoustic, Landmine Detection

1. INTRODUCTION

Based on the invariance of the wave equation to time reversal, systems have been built to use acoustic waves, and an array of transducers, to implement what is called a Time Reverse Mirror (TRM) [1]. In these systems a signal is recorded by an array of transducers, time-reversed and then re-transmitted into the medium. The signal propagates back through the same medium and refocuses on the source. TRMs have found application in medicine, nondestructive testing, underwater communication, and seismology, etc. These systems were used for detection, localization and sometimes destruction of passive targets. A recently developed method called D.O.R.T. provides a new approach to selective detection and focusing. This method is based on the decomposition of a time reversal operator [2]. In a system consisting of an array of N transducers, the time reversal operator is defined as $K^H(\omega)K(\omega)$, where ω is the frequency, and $K(\omega)$ is the transfer matrix of the array of N transducers obtained after performing N transmit-receive operations. It was shown that the time reversal operator can be diagonalized and that for ideally resolved scatterers of different reflectivities, each of its eigenvectors (corresponding to a nonzero eigenvalue) provides a signal to be applied to the transducers in order to focus on one of the scatterers. If the scatterers are assumed to be point-like, i.e., much smaller than the wave-length, then it was also shown that eigenvectors of the time-reversal operator are proportional to the Green's function (or impulse response) coming from the scatterers.

Subspace methods, like classical MUSIC have been used for quite some time to provide high resolution DOA estimates. In turn, these DOA estimates can be used to detect and localize targets. MUSIC is based on the eigenvectors of the covariance matrix obtained from data recorded on a passive sensor array. In [3,4] it was shown that the time-reversal operator can be interpreted as a covariance matrix used in passive array techniques. In [3] a MUSIC-based narrow-band imaging algorithm was presented for a homogenous medium. It was shown that the eigenvectors of the time-reversal matrix can play the role of eigenvectors of the covariance matrix. The rank of the time-reversal matrix was shown to be equal to the number of targets, and the eigenvectors can be used to form signal and noise subspaces. The signal subspace is spanned by the Green's function vectors from the targets, with noise subspace being orthogonal to this. Using the Green's function vector estimate as the steering

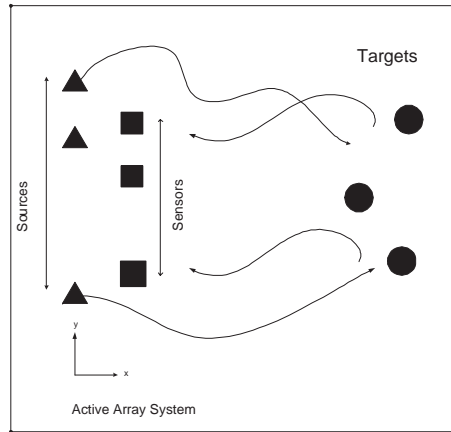


Figure 1. Active Array System

vectors, a pseudo-spectrum is computed, which peaks at the spatial positions of the targets.

In this paper, the equivalence between the time-reversal matrix and the covariance matrix used in standard array processing techniques will be exploited to produce a final image with improved cross-range and down-range resolution. Using the array model for near-field sources, a 2-D MUSIC based algorithm will be presented and will be shown to have excellent range resolution [8,9]. A FDTD elastic-wave simulation will be used to verify the results of the new algorithms [6]. The simulation will model an active acoustic/seismic array system with mines or mine-like targets in a vertically stratified soil.

2. FDTD BASED NUMERICAL SIMULATION SETUP

The numerical data is generated by using a FDTD model, with landmines acting as targets in a vertically stratified, inhomogeneous soil (see [6] which describes the interaction of buried mines with elastic waves in detail). The transmitted pulse is a differentiated Gaussian pulse centered at 450 Hz. The response matrix is populated by probing the medium using one transmitter at a time, and measuring the reflections at all the receivers. The forward traveling wave in each scan is removed at each receiver by time gating, so that only the reflected waves are processed. The test area is 165 cm \times 100 cm with mines buried at an average depth of approximately 2 cm. The active array system is shown in Fig. 1. The transducers are placed at the surface of the earth, covering an aperture of $(N - 1)d$ across y at constant x position, where d is sensor spacing. The spacing is usually $\frac{\lambda}{2}$, where λ is the wavelength corresponding to the maximum frequency, which is often much higher than the dominant frequency at which image is formed. This emulates an acoustic/seismic detection system which will be used in actual experiments. The results will be given for two cases, one with two similar targets at the same range from the sensors, and other with two different targets at two different ranges. The setup for both cases is given by following table:

	Case-1	Case-2
Number of sources	15	6
Number of receivers	23	15
Source spacing	6cm	9cm
Receivers spacing	4cm	4cm

In addition to the data collected in the above setup, another data set is collected by placing sensors across the x direction at constant y . This scan is used to obtain medium characteristics like wave velocity, wave number, and wavelength, etc., which is used for imaging and other algorithms. Reliable prior estimates of these parameters are very important for good resolution images. The algorithm to obtain the seismic/acoustic wave parameters is described in detail in [7].

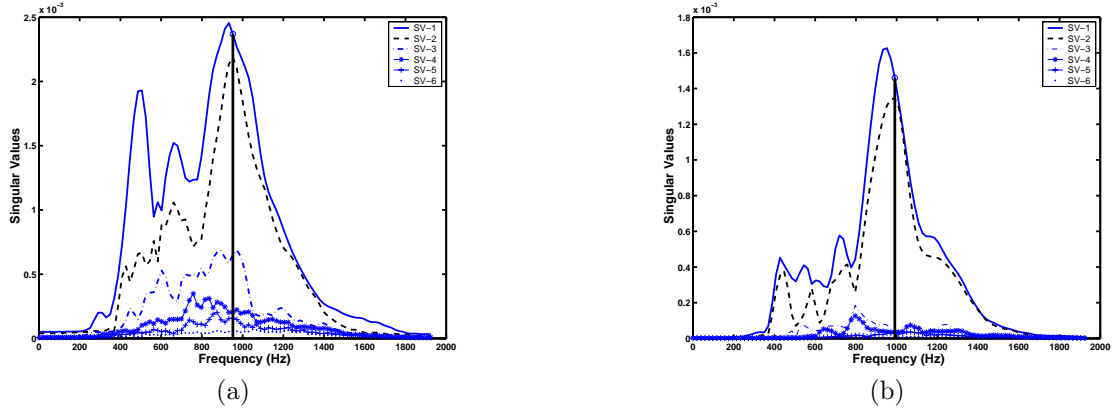


Figure 2. Singular values versus frequency. (a) Case-1 (b) Case-2

The plot of first six significant singular values of response matrix for both cases is shown in Fig. 2. Both plots show two big singular values larger than the rest indicating the two strong targets. The plot for case-1 also shows some other significant singular values. These additional values are related to the stronger target. The plots also show the single frequency at which the image plots are produced (vertical line). This frequency is chosen because the strength of the singular values is strongest at this frequency.

3. TIME REVERSAL MATRIX AND MUSIC BASED ALGORITHM

Consider an array of N_t transmitters located at \mathbf{x}_t , and an array of N_r receivers located at \mathbf{x}_r , where $\mathbf{x}_{t,r}$ are vectors of spatial positions in 2-D space. In our setup we assume $N_t \neq N_r$ and $\mathbf{x}_t \neq \mathbf{x}_r$, but it is possible have co-located transmitters and receivers. The transfer matrix $K(\omega)$ has the following form in terms of the Green's functions and scattering coefficients of the targets [3, 5],

$$K(\omega) = f(\omega) \sum_{j=1}^M \xi_j g(\mathbf{y}_j, \mathbf{x}_r, \omega) g^T(\mathbf{y}_j, \mathbf{x}_t, \omega) \quad (1)$$

where $f(\omega)$ is the Fourier transform of the transmitted pulse, ξ_j is the scattering coefficient of the j^{th} target, M is the number of targets, and \mathbf{y}_j is the position of j^{th} target in the 2-D plane. The matrix $K(\omega)$ is $N_t \times N_r$. The illuminating Green's vector g is given by

$$g(\mathbf{y}_j, \mathbf{x}, \omega) = [G(\mathbf{y}_j, \mathbf{x}_1, \omega), G(\mathbf{y}_j, \mathbf{x}_2, \omega), \dots, G(\mathbf{y}_j, \mathbf{x}_N, \omega)]^t \quad (2)$$

where G is a scalar Green's function, and \mathbf{x} is either the receiver or transmitter positions. With the assumption that there is no multiple scattering between the unknown targets, the rank of the transfer matrix is always less than or equal to the number of targets. The Singular Value Decomposition (SVD) of the transfer matrix is

$$K(\omega) = U(\omega) \Sigma(\omega) V^H(\omega) \quad (3)$$

where $\Sigma(\omega)$ is a diagonal matrix of real-valued singular values, and $U(\omega)$ and $V(\omega)$ are unitary matrices. If the targets are point-like, isotropic scatterers, with distinct reflectivities, and are well resolved by both the transmit and receive arrays, then there is one-to-one correspondence between the Green's functions of targets and the eigenvalues and eigenvectors. For extended targets like land mines, it appears that the eigenvectors are a linear combination of the Green's function vectors from the targets. The relation between eigenvalues and eigenvectors of time-reversal matrix and that of the transfer matrix $K(\omega)$ is given by the following normal equations [5]

$$[K^H(\omega)K(\omega)]V_i(\omega) = \sigma_i^2(\omega)V_i(\omega) \quad (4a)$$

$$[K(\omega)K^H(\omega)]U_i(\omega) = \sigma_i^2(\omega)U_i(\omega) \quad (4b)$$

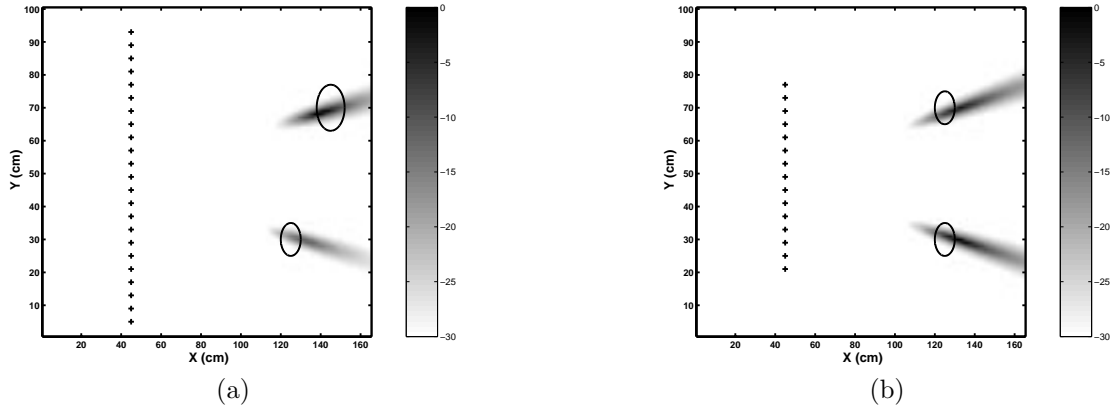


Figure 3. Single Frequency MUSIC Spectrum (a) Case-1 (b) Case-2

where $\sigma(\omega)$ are the diagonal elements of $\Sigma(\omega)$. Although either of these equations can be used as the definition for the time-reversal matrix, if the transmitters and receivers are at different spatial positions then (4a) and (4b) can be interpreted as related to receiver and transmitter subspaces respectively [5].

The eigenvalues and eigenvectors of the response matrix as given by (3) can be used to detect and localize targets. Specifically, the number of significant eigenvalues indicates the number of targets, i.e.,

$$\sigma_1 \geq \dots \geq \sigma_M \geq \sigma_{M+1} \approx \dots \sigma_N \approx 0 \quad (5)$$

where N can be N_r or N_t . To localize the targets we can use the eigenvectors of the response matrix and an estimate of the Green's function of the medium. The first M singular vectors $SV_1(\omega), \dots, SV_M(\omega)$ form an orthogonal basis of the M -dimensional signal subspace of \mathbb{C}^N , spanned by the illuminating vectors at the target locations $g(\mathbf{y}_1, \omega), \dots, g(\mathbf{y}_M, \omega)$, while the singular vectors $SV_r(\omega)$, for $M + 1 \leq r \leq N$ are orthogonal to this subspace [3]. If we can estimate the signal and noise subspaces of the time-reversal matrix, then a MUSIC-like algorithm can be formulated using the following principle: "if the Green's vector $g(\mathbf{y}^s, \omega)$ at a search point \mathbf{y}^s is orthogonal to the null-space of the time-reversal matrix then \mathbf{y}^s must be the position of the target, and the inner product of this Green's vector with the null-space is zero, as compared to when the test point is not at the target location." Mathematically, this can be expressed as

$$S_{MU}(\mathbf{y}^s, \omega) = \frac{1}{\sum_{i=M+1}^N |\langle SV_i(\omega)g(\mathbf{y}^s, \omega) \rangle|^2} \quad (6)$$

where $\langle \rangle$ denotes inner product. If we use (4a), then the singular vectors are the $V_i(\omega)$, but with (4b) they are the $U_i(\omega)$ vectors from the SVD [5]. Here we assume that the sources and receivers are not co-located, which is the case in our setup. For a 2-D space, the estimate of the Green's vector can be given via the zero-order Hankel function of the first kind as

$$G(\mathbf{r}, \mathbf{r}', \omega) = \frac{i}{4} H_0^{(1)}(k(\omega)|\mathbf{r} - \mathbf{r}'|) \quad (7)$$

The wave-number $k(\omega)$ can be estimated by using the processing given in [7], along with a forward scan of the test area. For a vertically layered, inhomogeneous soil, that processing will produce a multi-mode dispersion curve. The $k(\omega)$ value related to Rayleigh wave mode can be extracted and used for the Green's function estimate.

The single frequency MUSIC plot, using (6), for two cases is shown in Fig. 3. The problem with range resolution in this case is clearly visible, even though there is very good cross-range resolution. The reason for poor range resolution is that the Green's function doesn't change that much around the target point, and also the sensor array is one-dimensional, providing cross-range resolution only.

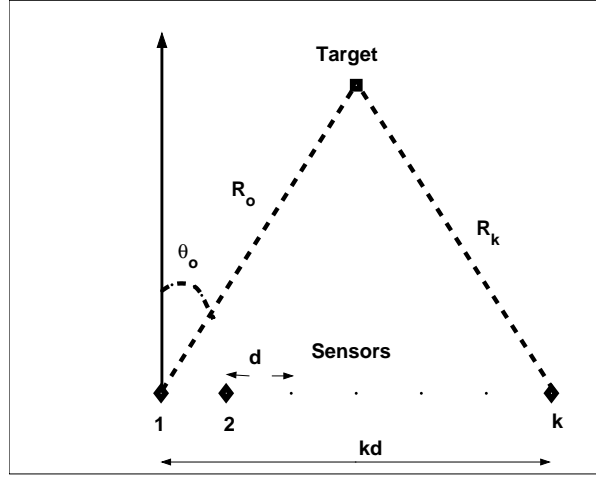


Figure 4. Near Field Array Setup

4. TIME REVERSAL MATRIX AND NEAR FIELD DOA AND RANGE ESTIMATES

In standard array processing several algorithms have been proposed to estimate the range and DOA parameters for near-field sources. For sources close to the array, the wavefront is no longer planar [9]. In [3, 4], it was proven that the time-reversal matrix can be interpreted as a covariance matrix used in standard passive array techniques. This interpretation leads to an imaging algorithm based on near-field geometry. Consider the near-field configuration shown in Fig. 4. The received signal at frequency ω is given by

$$X(\omega) = \mathbf{A}(r, \theta, \omega)S(\omega) + B(\omega) \quad (8)$$

where $S(\omega)$ is the source signal, $B(\omega)$ the noise matrix, and $\mathbf{A}(r, \theta, \omega)$ is $N \times M$ steering vector matrix, where N and M are numbers of sensors and targets, respectively. For near field sources, the i^{th} column of the steering vector matrix is given by [8, 9]

$$a(r, \theta, \omega) = [1, e^{j(\frac{2\pi}{\lambda(\omega)})(R_2 - R_o)}, \dots, e^{j(\frac{2\pi}{\lambda(\omega)})(R_N - R_o)}] \quad (9)$$

where d is the sensor spacing, and the range to the k^{th} sensor with respect to first reference sensor is

$$R_k = \sqrt{R_o^2 + k^2 d^2 - 2kdR_o \sin \theta_o}, k = 2, \dots, N \quad (10)$$

The most common methods of estimating the near field parameters is to use the Fresnel approximation to rewrite the signal in (10) as a chirp signal [9]. Then the imaging algorithm reduces to estimating the parameters of chirp signal. However, this method introduces errors when the target is extremely close to the array. An alternate approach is a 2-D MUSIC based approach like that used in [8]. In this method, the covariance matrix (from the array model) is given as

$$\mathbf{R}(r, \theta, \omega) = \mathbf{A}(r, \theta, \omega)\mathbf{R}_s(\omega)\mathbf{A}^H(r, \theta, \omega) + \sigma^2\mathbf{I} \quad (11)$$

where \mathbf{R}_s is the covariance of the sources and $\mathbf{A}(r, \theta, \omega)$ is the steering vector matrix defined in (8) and (10). It is sufficient to estimate the parameters (R_o, θ_o) for each source using the SVD of the covariance matrix. If the eigenvectors of the covariance matrix are arranged according to a descending order of singular values, then we form a noise eigenvector matrix as:

$$\mathbf{W}(\omega) = [\mathbf{u}_{M+1}, \dots, \mathbf{u}_N] \quad (12)$$

where M is the number of sources, and N the number of receivers. The rank of the covariance matrix is also M . To search for source locations, a 2-D orthogonality measure is constructed in the same manner as MUSIC.

$$\mathbf{P}(r, \theta, \omega) = \frac{1}{\mathbf{a}^H(r, \theta, \omega)\mathbf{W}\mathbf{W}^H\mathbf{a}(r, \theta, \omega)} \quad (13)$$

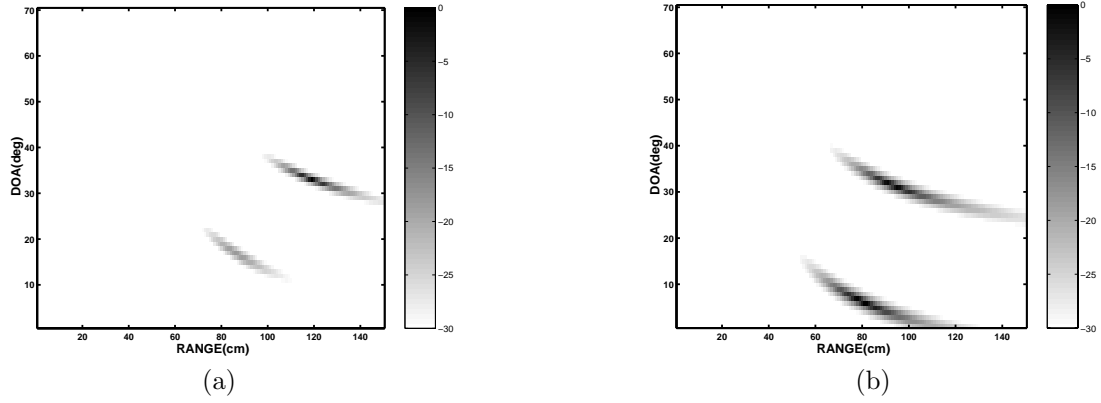


Figure 5. 2-D MUSIC Spectrum (a) Case-1(b) Case-2

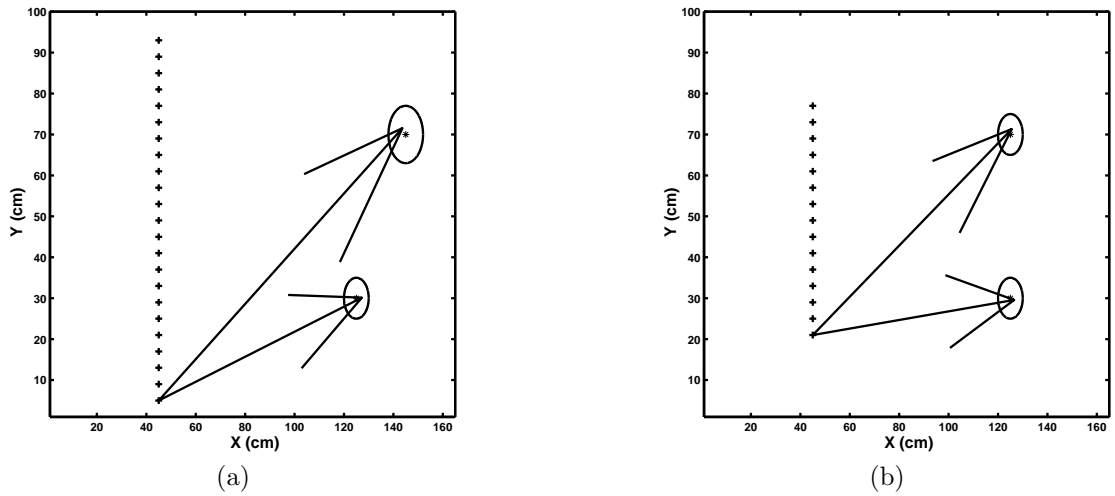


Figure 6. Near field DOA and Range Estimates (a) Case-1 (b) Case-2

The peaks of the spectrum $\mathbf{P}(r, \theta, \omega)$ will give the source locations, (r_k, θ_k) for $k = 1, 2, \dots, M$.

For an active array system, the time-reversal matrix at a single frequency is used as the covariance matrix estimate and then the same algorithm is carried out, using the singular value decomposition of $K^H(\omega)K(\omega)$. The steering vector is formed at a desired frequency by using (9). The spectrum obtained after applying the 2-D MUSIC algorithm is shown in Fig. 5. The spectrum peaks at the corresponding range and DOA values for two separate targets. These values can be extracted from the spectrum by searching for peak values and then adjusting these extracted values with respect to the reference sensor to get the absolute range and DOA. Plots of the near-field parameters are shown in Fig. 6.

A *range spectrum* can also be formed by using the following function,

$$S_R(\mathbf{y}^s, \omega) = \frac{1}{\left(\sum_{k=1}^N (R_k - \|\mathbf{x}_k - \mathbf{y}^s\|)^2 \right)^{\frac{1}{2}}} \quad (14)$$

where N and \mathbf{x}_k are the number and positions of receivers, and R_k is the range information given by (10). The denominator is the ℓ_2 norm between estimated range and the range calculated at each test point with respect to the array. This range spectrum should peak at the exact locations of the targets.

The link between time-reversal imaging and near-field DOA and range estimation can be proven by using the

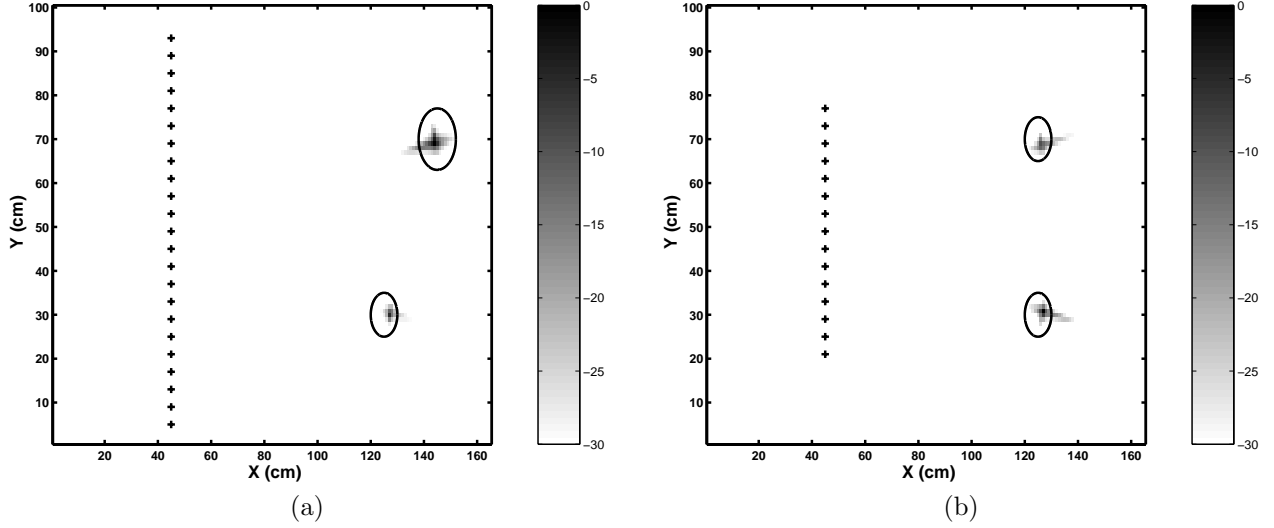


Figure 7. Combined MUSIC and Range Pseudo-Spectrum. (a) Case-1 (b) Case-2

similarity between the illuminating Green's vector given by (2) and the steering vector given by (9). Time-reversal imaging attempts to estimate the illuminating Green's vector given by:

$$g(\mathbf{y}_t, \mathbf{x}, \omega) = [G(\mathbf{y}_t, \mathbf{x}_1, \omega), G(\mathbf{y}_t, \mathbf{x}_2, \omega), \dots, G(\mathbf{y}_t, \mathbf{x}_N, \omega)] \quad (15)$$

where \mathbf{y}_t is the position of target and \mathbf{x} is the position of sensors. The asymptotic form of the scalar Green's function G in two dimensions can be written as a complex exponential:

$$G(r, r', \omega) = K e^{j\omega \frac{|r-r'|}{v}} = K e^{j\omega t'} \quad (16)$$

where K is a constant and t' is the time taken by a wave to travel the distance between r and r' . The Green's vector can be written as:

$$g(\mathbf{y}_t, \mathbf{x}, \omega) = [A_1 e^{j\omega t_1}, A_2 e^{j\omega t_2}, \dots, A_N e^{j\omega t_N}] \quad (17)$$

or with respect to the first sensor

$$g(\mathbf{y}_t, \mathbf{x}, \omega) \propto [1, B_2 e^{j\omega(t_2-t_1)}, \dots, B_N e^{j\omega(t_N-t_1)}] \quad (18)$$

using $(R_k - R_o) = (t_k - t_o)v$, where v is the wave velocity. In other words, equation (18) gives exactly the same form for the steering vector we had in (9), so we can conclude that time-reverse imaging is the same as finding the near-field source parameters.

5. COMBINED IMAGE BASED ON MUSIC AND NEAR FIELD PARAMETERS

Since MUSIC has good cross-range resolution, but poor range resolution, it must be combined with a spectrum obtained from parameters estimated for near-field sources. The final image will be the intersection of the spectra obtained in (6) and (14), that is

$$S(\mathbf{y}^s, \omega) = S_{MU}(\mathbf{y}^s, \omega) S_R(\mathbf{y}^s, \omega) \quad (19)$$

When both algorithms are combined using (19), the resulting spectrum is shown in Figs. 7 and 8 (mesh plot). This spectrum peaks at the correct position of the target, thus demonstrating that the problem with range resolution in MUSIC can be overcome by using it in conjunction with a near-field parameter estimator.

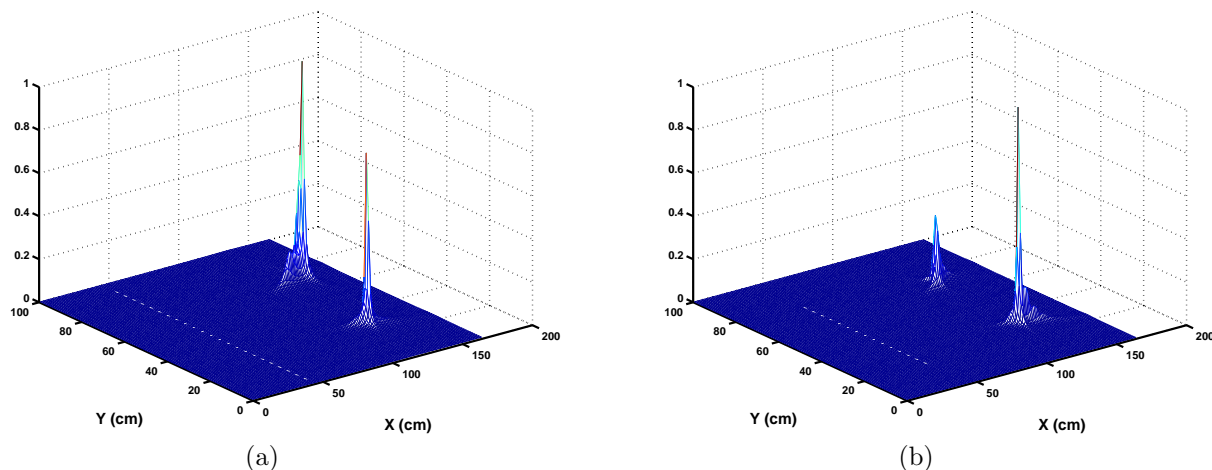


Figure 8. Combined MUSIC and Range Mesh Spectrum. (a) Case-1 (b) Case-2

6. CONCLUSION

The two algorithms proposed in this paper can be used to produce high-resolution images. The problems with range resolution in MUSIC-based algorithms can be overcome by using it in conjunction with a near-field source parameter estimator. The near-field parameters can be used to estimate the location of the target without triangulation, and in the absence of a Green's function estimate of the medium. Currently, work is in progress to build an experimental system based on the theory presented in this paper. In order to differentiate between clutter and actual mine targets, the resonance property of mines will be exploited, in addition to target reflections [6]. By combining the image obtained from using the reflection from the target with the resonance obtained by scanning the target area, mines should be more easily differentiated from clutter.

Acknowledgment

This work is supported by the U.S. Army Research Office under contract number DAAD19-02-1-0252.

REFERENCES

1. M. Fink, C. Prada, F. Wu, and D. Cassereau, "Self focusing in inhomogeneous media with time reverse acoustic mirrors," *IEEE Ultras. Symp. Proc.*, vol. 2, pp. 681–686, 1989
2. C. Prada, S. Manneville, D. Sponliansky, and M. Fink, "Decomposition of the time reversal operator: Detection and selective focusing on two scatterers," *J. Acoust. Soc. Am.*, 97, pp. 62–71, 1996
3. A. J. Devaney, "Super-resolution imaging using time-reversal and MUSIC," *J. Acoust. Soc. Am.*
4. C. Prada and J. Thomas, "Experimental subwavelength localization of scatterers by decomposition of the time reversal operator interpreted as a covariance matrix," *J. Acoust. Soc. Am.*, 114, pp. 235–243, 2003
5. S. K. Lehman and A. J. Devaney, "Transmission mode time-reversal super-resolution imaging," *J. Acoust. Soc. Am.*, 113, pp. 2742–2753, 2003
6. C. T. Schröder, "On the Interaction of Elastic Waves with Buried Land Mines: An Investigation Using the Finite-Difference Time-Domain Method," Ph. D. Dissertation, Georgia Institute of Technology, School of Electrical and Computer Engineering, Atlanta, GA, 2001.
7. M. Alam, McClellan, J. H., and Scott W. R., Jr., "Multi-Channel Spectrum Analysis of Surface Waves," *37th Asilomar Conference on Signals, Systems, and Computers*, Pacific Grove, CA, 2003.
8. Y. D. Huang and M. Barkat, "Near-field multiple source localization by passive sensor array," *IEEE Trans. Antennas Propagat.* vol. 39, pp. 968–974, July 1991.
9. A. L. Swindlehurst and T. Kailath, "Passive direction-of-arrival and range estimation for near-field sources," *Fourth Annual ASSP Workshop on Spectrum Estimation and Modeling*, pp. 123–128, 3–5 Aug. 1988.